Bioresource Technology 371 (2023) 128603

Contents lists available at ScienceDirect

Bioresource Technology

journal homepage: www.elsevier.com/locate/biortech

Process engineering strategy for improved methanol production in *Methylosinus trichosporium* through enhanced mass transfer and solubility of methane and carbon dioxide

Krishna Kalyani Sahoo, Ankan Sinha, Debasish Das *

Department of Biosciences & Bioengineering, Indian Institute of Technology, Guwahati, Assam 781039, India

HIGHLIGHTS

- Process engineering strategy for improved methanol production in *M. trichosporium*.
- Strategy targeted enhanced mass transfer (k_La) & solubility of CH_4 & CO_2.
- $k_La_{O_2}$: 98.5 h^{-1} & $k_La_{CH_4}$: 87.5 h^{-1} with 5 μm micro-sparger & 10 % v/v silicone oil.
- Biomass titer: 7.68 g/L & CH_4 fixation rate: 0.8 g/L d^{-1} in airlift reactor.
- Maximum methanol titer: 1.98 g/L in high-pressure stirred tank reactor at 4 bar.

GRAPHICAL ABSTRACT

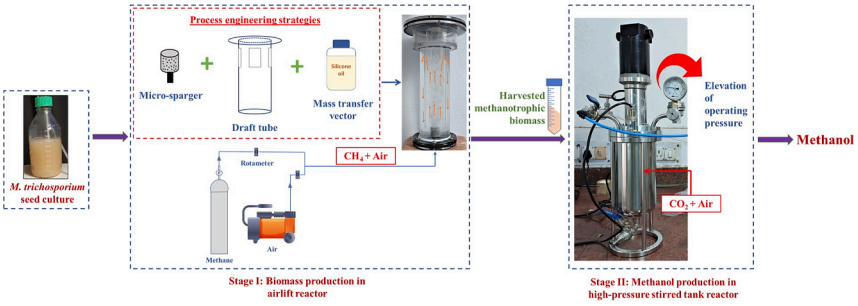

ARTICLE INFO

Keywords:
Methanotrophs
Methane
Carbon dioxide
High-pressure stirred tank reactor
Methanol

ABSTRACT

Methanol was produced in a two-stage integrated process using *Methylosinus trichosporium* NCIMB 11131. The first stage involved sequestration of methane to produce methanotrophic biomass, which was utilized as biocatalyst in the second stage to convert CO_2 into methanol. A combinatorial process engineering approach of design of micro-sparger, engagement of draft tube, addition of mass transfer vector and elevation of reactor operating pressure was employed to enhance production of biomass and methanol. Maximum biomass titer of 7.68 g/L and productivity of 1.46 g/L d^{-1} were achieved in an airlift reactor equipped with a micro-sparger of 5 μm pore size, in the presence of draft tube and 10 % v/v silicone oil, as mass transfer vector. Maximum methane fixation rate was estimated to be 0.80 g/L d^{-1}. Maximum methanol titer of 1.98 g/L was achieved under an elevated operating pressure of 4 bar in a high-pressure stirred tank reactor.

1. Introduction

The emission of greenhouse gases, such as methane and carbon dioxide, has been rising tremendously. The global energy sector itself has resulted in the emission of 36.3 billion tonnes of CO_2, and 135 million tonnes of methane, which accounts for only 40 % of the total anthropogenic methane emission (IEA, 2022; Global Methane Tracker, IEA, 2022). Hence, researchers are striving to combat the issue by exploring ways to sustainably convert these noxious compounds into liquid fuels and other value-added chemicals. Although, there are numerous

* Corresponding author.
E-mail address: debasishd@iitg.ac.in (D. Das).

https://doi.org/10.1016/j.biortech.2023.128603
Received 25 November 2022; Received in revised form 6 January 2023; Accepted 7 January 2023
Available online 9 January 2023

chemical methods to catalytically convert the greenhouse gases into useful chemicals, these chemical routes are constrained by the requirement of high-cost catalysts, extreme operating conditions such as high pressure and temperature, and release of noxious by-products (Sahoo et al., 2022, 2021). There have been reports on application of gas fermentation technology involving microorganism-driven biological routes to convert gaseous substances *e.g.,* carbon dioxide, methane and carbon monoxide into different high-value products such as ethanol (Tang et al., 2021), succinic acid (Amulya et al., 2020), lipids and single-cell proteins (Rasouli et al., 2018), poly-β-hydroxybutyrate (Zhang et al., 2018, 2017) and bio-hydrogen (Zhao et al., 2011). From a contextual perspective, methanotrophs, a class of Gram-negative, methane oxidizing bacteria, are being explored as noble platform to produce methanol (a potential fuel). Methanotrophs uptake methane as an obligate source for the derivation of carbon and energy. Methane is further oxidised into methanol, formaldehyde, formic acid, and CO_2 through sequential catalysis by intracellular enzymes namely, methane monooxygenase (MMO), methanol dehydrogenase (MDH), formaldehyde dehydrogenase and formate dehydroagenase, respectively (see supplementary materials). Except MMO, the set of other three enzymes are reversible in nature. Authors have reported methanol production through biological methane oxidation catalysed by MMO (Duan et al., 2011; Patel et al., 2020a). However, the methanol produced gets further oxidised into formaldehyde, formate and carbon dioxide by MDH and other enzymes, thereby, reducing the methanol titer. To overcome this, the activity of MDH is blocked through the addition of MDH inhibitor into the cultivation media. For example, Patel et al. (2016b) have demonstrated the effect of $MgCl_2$, EDTA, NH_4Cl, and NaCl, as MDH inhibitors for methanol production in *Methylosinus sporium*. Also, formate is supplemented as a NADH source, which acts as a cofactor for the functioning of soluble MMO. Alternatively, certain methanotrophs (*e.g., M. trichosporium* and *M. sporium*) have been reported as biocatalysts for methanol production through biological CO_2 reduction (Patel et al., 2016a; Sahoo et al., 2022). CO_2 being the metabolic end-product, when fed to the cells in excess concentration, drives the equilibrium in reverse direction. Owing to the irreversible nature of the MMO, this route leads to the extracellular secretion of methanol as the end-product. The reduction of CO_2 is powered by the presence of PHB reserves, which act as a source of reducing equivalent in addition to NADH (Xin et al., 2007). Therefore, the conversion of methane and CO_2 into methanol adopt different routes. While the methanol production from biological oxidation of methane requires higher MMO activity coupled with the inhibition of MDH activity; methanol production from biological reduction of CO_2 requires higher activity of formate dehydrogenase, formaldehyde dehydrogenase and methanol dehydrogenase, without any involvement of MMO. MMO oxidises methane into methanol. Hence, the activity of MMO in presence of methane has been correlated to methanol production, since the methanol titer decreases with the decrease in MMO activity (Patel et al., 2020a, 2020b). However, the presence of CO_2 is known to shift the equilibrium of methanotrophic metabolic reaction in reverse direction, thereby rendering the "irreversible enzyme MMO" non-functional (Sahoo et al., 2021).

Methanol production from greenhouse gases overcomes the problem of biomass limitation as is suffered in case of first- and second-generation biofuel production processes (*e.g.*, bioethanol, biodiesel), which rely on agricultural crops or lignocellulosic feedstocks (Verhelst et al., 2019). Moreover, unlike other microbial processes, which utilize costly carbon sources such as glucose, fructose, xylose, etc. as substrates, this process only uses waste greenhouse gases (CO_2 and/or CH_4), thereby reducing the operational expenses (Sahoo et al., 2021). Sahoo et al. (2022) reported a two-stage integrated process for methanol production. The process involves utilization of methane in the first stage to produce methanotrophic biomass, while carbon dioxide is utilized in the second stage to produce methanol using the biomass as biocatalyst. Also, researchers have adopted recent strategies in methanol production by methanotrophs using low-cost feed (biogas) derived through anaerobic digestion and dark-fermentation of biowastes as an alternative to pure gas (Patel et al., 2023, 2022). However, one of the key challenges in the biological process for methanol synthesis from methane and CO_2 is the low titer of the biomass and methanol, which is primarily attributed to inferior mass transfer rates and limited solubility of the gaseous substrates in the liquid medium (Sahoo et al., 2022, 2021). Process engineering strategies from the perspective of suitable reactor configuration and design, supplementation of exogenous mass transfer vectors and application of elevated pressure, are potential approaches towards combating the hurdles associated with limited mass transfer and solubility. Airlift reactors are considered to be advantageous over other reactor configurations attributed to better mixing and mass transfer, greater liquid recirculation and gas hold-up, absence of mechanical agitation and lower power requirement (Doran, 1995). Researchers have reported the application of airlift bioreactors for the cultivation of methanotrophic biomass towards the enhancement of methane biodegradation and methanol production through direct oxidation of methane (Ghaz-Jahanian et al., 2018; Rocha-Rios et al., 2011). Reactor design aspects, especially from the point of view of design of sparger and configuration of draft tube in an airlift reactor hold a significant importance in defining the reactor performance characteristics when the reactions occurring inside the system are limited by mass transfer phenomena. Spargers predominantly play key role in generation and dispersion of gases in the form of bubbles. In contrast to conventional spargers which generate coarse bubbles, micro-spargers lead to generation of fine microbubbles, characterized by higher specific interfacial area (larger ratio of surface area to volume) and thus, offers improvement in volumetric mass transfer coefficient (Hanotu et al., 2017). Another key distinguishing feature of an airlift reactor is the draft tube. Draft tubes have been reported to improve circulation and axial mixing inside the reactor. Moreover, the draft tube induces a unidirectional pattern of liquid circulation leading to unidirectional movement of bubbles, and consequent reduction in bubble coalescence (Duan and Shi, 2014).

The limited solubility of gaseous substrates in liquid medium is yet another hurdle associated with gas fermentation. The maximum solubility of CO_2 in water 0.874 mol percent at a temperature and pressure of 373.15 K and 5.03 MPa, respectively (Lucile et al., 2012). Whereas, at the same temperature, the highest solubility of methane in water is 6×10^{-3} mole percent at a pressure of 10 MPa (Pruteanu et al., 2017). Mass transfer vectors, a class of organic solvents are reported to enhance the solubility of gaseous substances in the liquid medium. For instance, paraffin oil and silicone oil are reported to enhance the bioavailability of methane and oxygen to the cells (Han et al., 2009; Rocha-Rios et al., 2009). This could be attributed to the fact that relative to aqueous mineral salt media, mass transfer vectors possess greater affinity for oxygen and methane. This increased dissolution of gases upon vector supplementation in the media has been reported to have positive influence not only on the production of biomass (Han et al., 2009), but also on methanol (Patel et al., 2020b). For instance, Patel et al. (2020b) reported 1.7-fold increment in methanol production by adding methane vectors to methanotrophic culture as compared to control. Similarly, Patel et al. (2023) reported a residual methanol production efficacy of 28.3 % in presence of paraffin oil as methane vector, as compared to 13.4 % in control, after 6 cycles of biomass reuse. Moreover, the supplementation of methane vectors has shown to enhance the biocatalytic activity of MMO. For instance, Patel et al. (2023) reported residual MMO activity of 37.4 % in presence of paraffin oil relative to 16.9 % in case of control after 6 cycles of biomass reuse. Furthermore, elevated operating pressure has been reported to be a suitable strategy towards enhancing the solubility of gaseous substrates in various microbial gas fermentation systems (Van Hecke et al., 2019). However, the lower mass transfer and limited solubility of methane and carbon dioxide in methanotrophic gas fermentation still presents a major bottleneck, exerting a limiting impact on the titers and productivities of biomass and methanol.

The present study addresses the key challenges of bioavailability of

methane and carbon dioxide to methanotrophic bacteria for their conversion into methanol. A combinatorial approach of design of micro-sparger, engagement of draft tube and use of mass transfer vector was employed to achieve improved mass transfer and solubility of methane and in turn, increased titer of *Methylosinus trichosporium* biomass as biocatalyst. Further, conversion of carbon dioxide to methanol was carried out under elevated operating pressures in a customized high-pressure stirred tank reactor to achieve better solubility of carbon dioxide and in turn improved methanol titer. The employment of these process engineering strategies resulted in increments of 126 %, 148 % and 241 %, in biomass titer, methane fixation rate and methanol titer, respectively, as compared to the previous study in semi-batch stirred tank reactor (Sahoo et al., 2022).

2. Materials and methods

2.1. Organism and culture conditions

Methylosinus trichosporium NCIMB 11131 was obtained from National Collection of Industrial Food and Marine Bacteria, and was grown on nitrate mineral salt (NMS) medium containing (g L^{-1}): KNO_3 (1.0), $Na_2HPO_4{\cdot}12H_2O$ (0.306), KH_2PO_4 (0.111), $MgSO_4{\cdot}6H_2O$ (1.0), $CaCl_2$ (0.2), Fe-EDTA (0.0038) and $Na_2MoO_4{\cdot}2H_2O$ (0.00026). Trace metal solution (1 mL) comprising of (g L^{-1}): $CuSO_4{\cdot}5H_2O$ (0.15), $FeSO_4{\cdot}7H_2O$ (0.375), $ZnSO_4{\cdot}7H_2O$ (0.3), H_3BO_3 (0.01125), $CoCl_2{\cdot}6H_2O$ (0.0375), EDTA di-sodium salt (0.1875), $MnCl_2{\cdot}4H_2O$ (0.015) and $NiCl_2{\cdot}6H_2O$ (0.0075) was added to the media. Medium pH was calibrated to 6.8 by adding 1 M H_2SO_4 and 1 M NaOH. Milli-Q water (18 MΩ) was used to prepare all the reagents. All the chemicals were of analytical grade and bought from Himedia and other commercial suppliers. Inoculum preparation was carried out as described previously (Sahoo et al., 2022) by cultivating the cells in 100 mL of NMS medium in customized air-tight bottles. Cultures were incubated in a shaker incubator (ORBITEK, Scigenics Biotech) at 30 °C and 150 rpm with intermittent sparging of air and methane. The cells from mid-log phase culture with an optical density (A_{600}) of 5.0 were used as inoculum (10 % v/v concentration) for all experiments.

2.2. Growth of methanotrophs using methane as sole carbon source in customized airlift bioreactor

Generation of methanotrophic biomass was carried out in the first stage of two-stage integrated process using methane as sole carbon source. The strain *M. trichosporium* was evaluated for its growth using micro-sparger with varying pore size, use of draft tube and presence of mass transfer vectors. All the experiments were carried out in customized airlift bioreactor using optimized NMS media at room temperature and the culture was sparged continuously with methane-air mixture. The concentration of methane in the inlet gas stream and the gas flow rate were maintained at 2.5 % v/v and 0.5 vvm, respectively (Sahoo et al., 2022). Samples were collected at an interval of 8 h to obtain dynamic profiles of growth. k_La for oxygen and methane were estimated as described later in the Section 2.2.3. Methane fixation rate was calculated using Eq. (1) (Sahoo et al., 2022)

$$\text{Methane fixation rate } \left(\text{g L}^{-1}\text{d}^{-1}\right) = \text{P}_x \times \text{E}_c \times \left(\frac{16}{12}\right) \quad (1)$$

where P_x is the biomass productivity (g/L d^{-1}), E_c is the content of elemental carbon in the biomass. 16 and 12 are molecular weight of methane and carbon, respectively.

2.2.1. Design of airlift reactor

A laboratory-scale (Total volume: 700 mL, working volume: 500 mL) internal loop airlift reactor was constructed from clear polycarbonate sheet with a total height of 23.5 cm, and the inner diameter of the column being 7 cm (Fig. 1a). A draft tube with a total height of 22.5 cm and inner diameter of 4 cm was mounted coaxially attached to the headplate. Three rectangular openings (5 cm × 1.5 cm) were provided in the upper portion of the draft tube, and a clearance of 1 cm between the lower rim of the draft tube and the bottom of the reactor column for allowing the circulation of the liquid through the riser and the downcomer sections. The reactor column contained a gas separator section at the top with a height of 2.5 cm and an inner diameter of 10 cm to facilitate liquid recirculation and bubble disengagement. Gaseous substrates (mixture of air and methane) were introduced into the reactor column through a removable sintered metal gas sparger attached to the centre of the reactor bottom below the draft tube. The cross-sectional channel inside the draft tube, and the annulus between the draft tube and the reactor column, were used as the riser and the downcomer, respectively. Ports were provided on the headplate for exhaust and placement of DO probe.

2.2.2. Effect of sparger pore size, draft tube and mass transfer vector on growth of the strain

Sintered metal micro-spargers with a height of 2.67 cm and diameter of 1.5 cm were customized for the airlift reactor for the given pore sizes: 5, 10, 40, 70 and 100 μm. The growth characterisation of the strain was carried out in the customized airlift reactor equipped with micro-spargers of varying pore sizes (5–100 μm). In the next step, the growth characterization was performed in the absence of draft tube, where draft tube mounting was not provided in the headplate. The effect of mass transfer vector was assessed by supplementing varying concentrations (5–10 % v/v) of two different organic solvents such as paraffin oil and silicone oil in the cultivation medium.

2.2.3. Estimation of k_La for oxygen and methane

Volumetric mass transfer coefficient for oxygen ($k_La_{O_2}$) was estimated using the gas out–gas in unsteady-state mass balance method for oxygen, as described earlier by Ghaz-Jahanian et al. (2018). Change in the concentration of oxygen in the culture media was measured using dissolved oxygen (DO) probe (METTLER TOLEDO, Switzerland). Initially, deoxygenation of NMS media was carried out by purging nitrogen into the reactor until the DO concentration dropped to zero. Subsequently, the media was reoxygenated by purging air into the reactor at a uniform flow rate of 0.5 vvm. The variation in DO concentration (C_t) during reoxygenation was recorded as a function of time, and continued until the DO concentration reached a steady-state value ($\overline{C}$). The rate of change in DO concentration is equal to the rate of oxygen transfer from gas to liquid. Therefore,

$\frac{dC_t}{dt} = k_La_{O_2}$ ($\overline{C}$-C_t) (2)where C_t is the DO concentration at time t, and ($\overline{C}$) is the steady-state DO concentration.

Integrating Eq. (2) between t_1 and t_2 results in:

$k_La_{O_2} = \frac{\ln\frac{(\overline{C}-C_{t_1})}{(\overline{C}-C_{t_2})}}{(t_2-t_1)}$ (3)where C_{t_1} and C_{t_2} are the DO concentrations are time points t_1 and t_2, and $k_La_{O_2}$ is the slope obtained by plotting $\ln\frac{(\overline{C}-C_{t_1})}{(\overline{C}-C_{t_2})}$ against time. The volumetric mass transfer coefficient for methane ($k_La_{CH_4}$) was calculated using the value of $k_La_{O_2}$ as per the equation reported by Ghaz-Jahanian et al. (2018) for upcoming bubbles in airlift bioreactor:

$$k_La \propto \left(\frac{1}{V_m}\right)^{0.3} \quad (4)$$

where V_m is the molecular volume, which is 25.6 and 37.9 cm^3 $gmol^{-1}$ for oxygen and methane, respectively. Thus, based on the molecular volumes of oxygen and methane, $k_La_{CH_4}$ was calculated from $k_La_{O_2}$ using Eq. (5).

$$k_La_{CH_4} = 0.889\ k_La_{O_2} \quad (5)$$

It should be noted that, Eq. (4) is based on the assumptions that

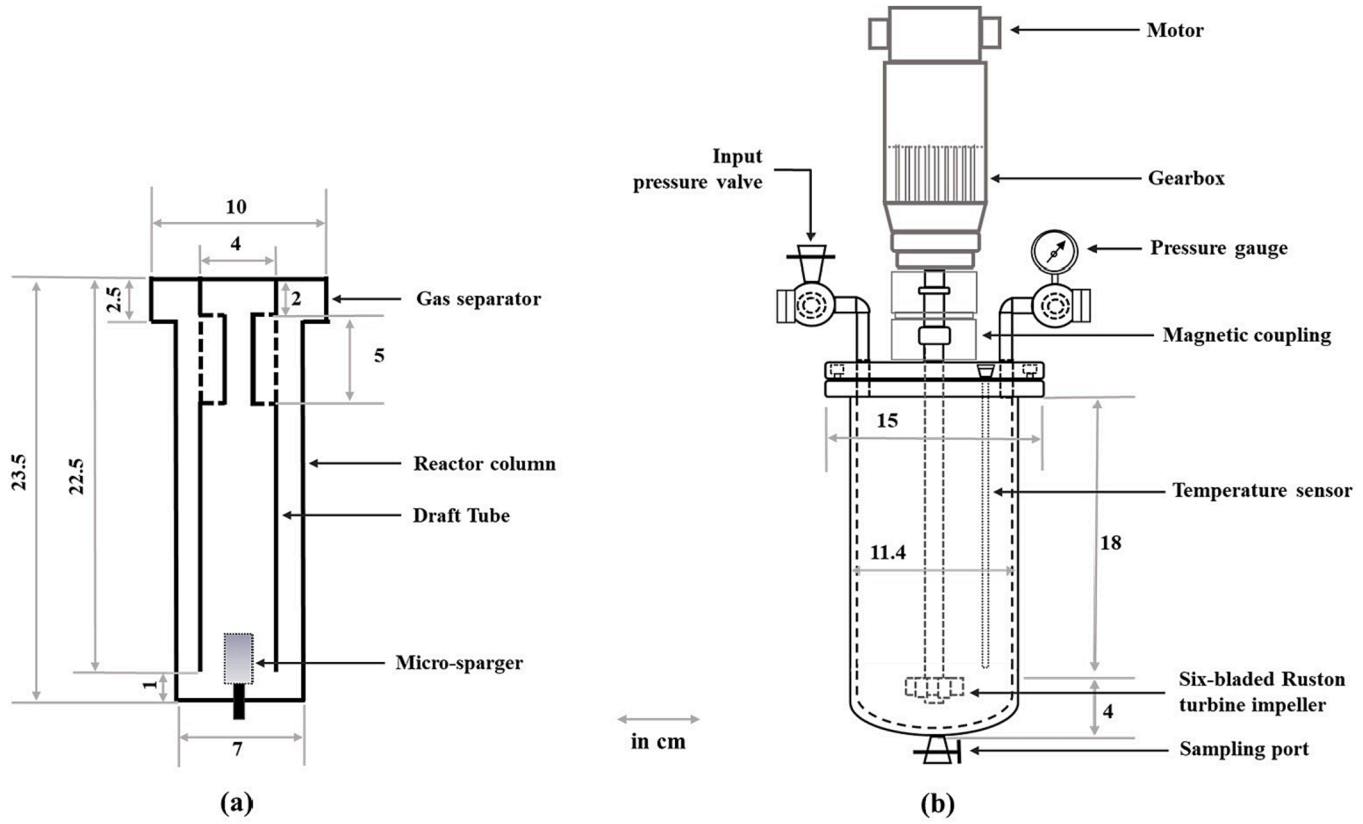

Fig. 1. Schematic diagram of (a) internal loop airlift reactor and (b) high-pressure stirred tank reactor. All the dimensions are in centimetres.

$k_L a_{CH_4}$ varies as k_L, and the interfacial area does not depend on the gas type, which may not be true for some gases (*e.g.*, H_2).

2.3. Conversion of carbon dioxide into methanol using biomass as biocatalyst: Effect of operating pressure

The methanotrophic biomass generated in the first stage of the integrated process was used as biocatalyst for conversion of carbon dioxide to methanol under varying operating pressure. A laboratory-scale stirred tank reactor with a maximum working volume of 1.2 L was fabricated using SS-316-grade stainless steel with a total height of 22 cm and an outer diameter of 11.4 cm (Fig. 1b). The reactor was designed to withstand pressure as high as up to 10 bar. The reactor was equipped with six-bladed Rushton disk turbine impeller for efficient mixing, temperature detector, pressure gauge, pressure release valve and ports for gas feeding and sampling. The culture was assessed for methanol production under varying headspace pressure of 1, 2, 3, 4 and 5 bar. The CO_2 concentration in the headspace and liquid to headspace volume ratio were maintained at 50 % v/v and 10:90, respectively, based on the results obtained from previous study (Sahoo et al., 2022). The desired pressure in the headspace was achieved by injecting a mixture of CO_2 and air in the beginning of the batch using rotameters. The reactor was operated at room temperature and 150 rpm. In this step, the harvested biomass (3.39 g L^{-1}) was resuspended in 20 mM phosphate buffer (pH 6.8) containing 5 mM $MgCl_2$ (Sahoo et al., 2022). Sampling was carried out at regular time intervals to obtain dynamic profiles for methanol production and growth.

2.4. Analytical methods

Cell growth was estimated by measuring the absorbance at 600 nm (A_{600}) using UV–Vis spectrophotometer (Cary Series 100, Agilent Technologies). The absorbance values were converted into dry cell weight (DCW) using the correlation, one optical density = 0.42 g dry cells L^{-1} (R^2 = 0.99). Sample was centrifuged (HERAEUS, MULTIFUGE X3R Centrifuge, Thermo Scientific) at 10,000 rpm for 15 min to obtain cell-free supernatant for the estimation of methanol titer. Methanol concentration in the sample was estimated by high performance liquid chromatography (HPLC) (Ultimate 3000, Dionex, Thermofisher Scientific, Germany) in refractive index detector (RID) using Rezex ROA column (300 × 7.8 mm, Phenomenex) and 0.005 N H_2SO_4 as mobile phase at a flow rate of 0.5 mL min^{-1}. Refractive index detector and column oven were kept at 37 °C and room temperature, respectively. Elemental composition (C, H, and N) of the biomass was obtained using CHNS analyser (EuroEA Elemental Analyser). Statistical significance was evaluated through one-way ANOVA with the help of MINITAB software at 95 % confidence interval.

3. Results and discussion

Methanol production was carried out in a sequential two-stage integrated process, as described earlier (Sahoo et al., 2022). In brief, the first stage involved production of methanotrophic biomass through utilization of methane as carbon source, while the second stage encompassed reduction of carbon dioxide to methanol using harvested methanotrophic biomass as biocatalyst. The process, however, is constrained by poor mass transfer rates and limited solubility of the methane and carbon dioxide in the liquid medium; thereby imposing limit on the titers of biomass and methanol. To that end, the current study presents a combinatorial process engineering approach towards obtaining improved biomass and methanol production.

3.1. Process engineering strategies for improved production of methanotrophic biomass in the first stage

The first stage of methanotrophic biomass production was carried

out in customized airlift bioreactor. Certain approaches from the perspective of reactor design, such as, use of micro-sparger and placement of draft tube, along with another process engineering strategy, *i.e.*, exogenous addition of mass transfer vector, were applied to the airlift reactor. Subsequently, characterisation was carried out to evaluate the consequent impact on k_La, biomass titer, biomass productivity and methane fixation rate.

3.1.1. Evaluation of the effect of varying pore sizes of micro-sparger

Design of the sparger plays a critical role in delineating the performance characteristics of airlift reactors, where there are no other moving parts to ensure adequate mass transfer of gaseous substrates in liquid media. In this regard, the pore size of the sparger holds significant importance, as the size of the pores on sparger regulate the size of the bubbles generating thereof, which in turn impact the volumetric mass transfer coefficient based on the characteristic interfacial area of the generated bubbles. To that end, characterisation of the organism was carried out using micro-spargers of various pore sizes ranging from 5 to 100 μm. Biomass titer was found to increase linearly from 4.54 ± 0.16 to 6.4 ± 0.26 g/L with the decrease in pore size of the micro-sparger from 100 to 5 μm (Fig. 2a). Similarly, the highest k_La for oxygen and methane of 78.1 ± 1.6 and 69.4 ± 1.4 h^{-1}, respectively, were obtained using the micro-sparger of 5 μm pore size (Fig. 2b), which was a 27-fold improvement over the values of k_La obtained using 100 μm micro-sparger. Furthermore, the maximum biomass productivity and methane fixation rate with 5-μm micro-sparger were estimated to be 1.27 ± 0.04 and 0.69 ± 0.02 g/L d^{-1}, respectively (Fig. 2c). Spargers with larger pore sizes are known to generate larger or coarse bubbles associated with lower volumetric mass transfer coefficient (Hanotu et al., 2017; Lukić et al., 2017). On the other hand, with the reduction in the pore size, micro-spargers (with pore sizes in the range of micrometres) generate even finer microbubbles, characterized by higher specific interfacial area (larger ratio of surface area to volume), leading to improvement in k_La, lower probability of bubble coalescence, and greater residence time inside the reactor. Moreover, in contrast to coarse bubbles, microbubbles are known to impart greater degree of aggregate convective force, consequently leading to a thoroughly mixed homogenous liquid phase (Hanotu et al., 2017). AL-Mashhadani et al. (2015) reported that the reduction in the size of microbubbles promoted downward penetration of gas bubbles through an increased vertical depth into the downcomer section, owing to an intensification in the downward drag force relative to the buoyant force, thus inducing greater liquid recirculation and mixing efficiency. Therefore, the improvement in biomass titer, biomass productivity and methane fixation rate with the decrease in the pore size of the micro-sparger could be attributed to the increase in mass transfer and mixing with 5-μm micro-sparger, and the consequent upsurge in the availability of methane to the cells.

Researchers have outlined the effect of sparger structure and pore size on volumetric mass transfer coefficient in different types of airlift reactors. Luo et al. (2011) reported that in an internal loop airlift reactor while a 2-orifice nozzle (pore diameter: 2.6 mm) resulted in a k_La of 0.0018 s^{-1} (6.48 h^{-1}), a 4-orifice nozzle (pore diameter: 1.84 mm) resulted in a much higher k_La of 0.0023 s^{-1} (8.28 h^{-1}), suggesting that spargers with lesser pore sizes generate bubbles with lower mean diameter, and thus are associated with greater specific interfacial area and liquid circulation velocity, consequently leading to a relatively higher k_La. A similar study in an external loop airlift reactor reported 550 % improvement in k_La with a sinter plate sparger with mean pore diameter of 115 μm, as compared to a single orifice sparger with a pore size of 4 mm (Lukić et al., 2017). Sintered-type spargers reportedly produce very stable and smaller bubbles, and generate a bubbly flow regime along with prolonged bubble residence time, resulting in an improved k_La(Lukić et al., 2017). The findings of the present study align well in accordance with these literature reports, thus signifying the importance of smaller pore sizes in spargers towards enhancing the mass transfer in airlift reactors.

3.1.2. Evaluation of the effect of engagement of draft tube

In order to evaluate the effect of engagement of draft tube in airlift reactor, the growth of the organism was assessed with and without the placement of draft tube in the reactor equipped with 5-μm micro-sparger. The biomass titer was found to decrease by 8.59 % in the absence of the draft tube, *i.e.*, from 6.4 ± 0.26 g/L to 5.85 ± 0.18 g/L (Fig. 3a). Additionally, the values of $k_La_{O_2}$ and $k_La_{CH_4}$ were observed to decrease by 27.4 % each (Fig. 3b). Likewise, biomass productivity and methane fixation rate showed decrements of 13.3 % and 13.4 %, respectively, in the absence of the draft tube (Fig. 3c). These experimental observations emphasized the indispensable requirement for placement of draft tube in the airlift reactor towards achieving improved mass transfer coefficient, and consequent augmentations in biomass titer, biomass productivity and methane fixation rate.

The presence of draft tube in an airlift reactor divides the vessel longitudinally into riser and downcomer sections. Bubbles rise inside the riser section causing vertical flow of the liquid in upward direction. This upward force exerted in the riser section is counter-balanced by vertical downflow of the liquid inside the downcomer section (Duan and Shi, 2014). The up-flow and downflow of the liquid result in efficient circulation and mixing of the liquid. Improved liquid circulation imparts a uniform velocity to the bubbles causing them to traverse in uniform direction. This kind of flow pattern has been reported to consequently minimize the probability of bubble coalescence and improve the k_La. Researchers have highlighted the significance of draft tube in controlling the mass transfer and the hydrodynamic behaviour of airlift reactor. For instance, Hekmat et al. (2010) outlined that draft tube facilitated the circulation of liquid through a complete cycle inside the reactor, and

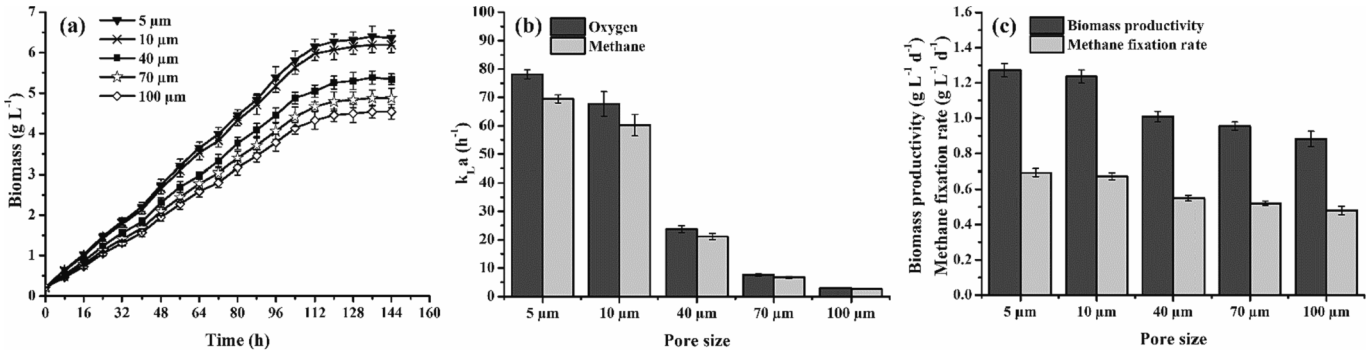

Fig. 2. (a) Biomass titer, (b) volumetric mass transfer coefficient for oxygen ($k_La_{O_2}$) and volumetric mass transfer coefficient for methane ($k_La_{CH_4}$) and (c) biomass productivity and methane fixation rate obtained in airlift reactor with varying pore sizes of micro-sparger. Significant differences ($p \leq 0.05$) were noted through statistical analysis using one-way ANOVA.

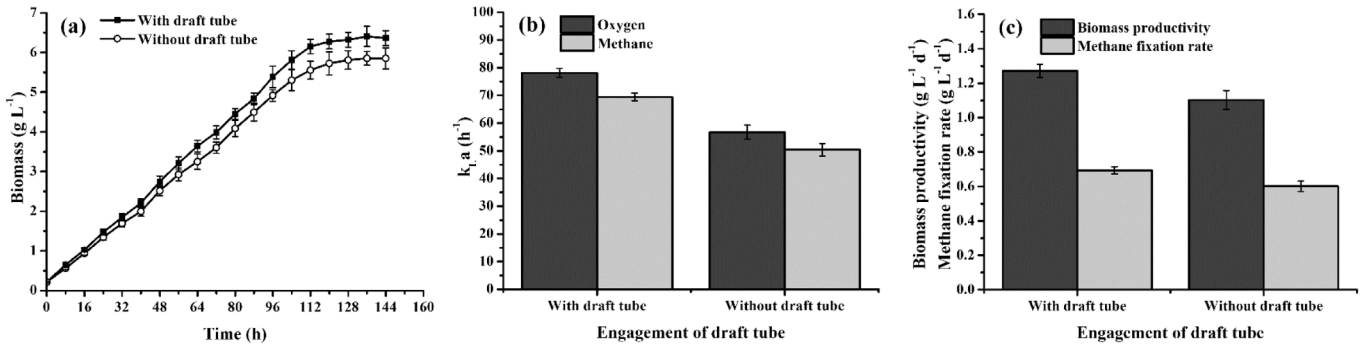

Fig. 3. Effect of draft tube on (a) biomass titer, (b) volumetric mass transfer coefficient for oxygen ($k_La_{O_2}$) and volumetric mass transfer coefficient for methane ($k_La_{CH_4}$) and (c) biomass productivity and methane fixation rate in airlift reactor equipped with micro-sparger of 5 μm pore size. Significant differences ($p \leq 0.05$) were noted through statistical analysis using one-way ANOVA.

decreased the quantity of liquid hold-up in the gaseous phase of the reactor, and thus cutting down the requirement for gas–liquid separation steps for the products exiting the reactor outlet. Li et al. (2020) reported that the geometric configuration of draft tube has notable influence on gas hold-up, gas residence time and mass transfer, which in turn regulate the power efficiency of airlift reactors. Authors have even reported 40–100 % improvement in k_La with the installation of draft tube in conventional mechanically agitated stirred tank reactor (Lueske et al., 2015). These literature reports in line with the present experimental results fairly justify the role of draft tube in airlift reactors for attaining improved performance.

3.1.3. Evaluation of the effect of supplementation of mass transfer vector

To overcome the limited solubility of methane and oxygen in NMS media, and increase their bioavailability to the cells, the media was supplemented with mass transfer vectors. *M. trichosporium* growth was evaluated under 0–10 % v/v of paraffin oil and silicone oil. While, the absence of mass transfer vector (control) resulted in 6.4 ± 0.26 g L^{-1} of biomass titer, the addition of 5 % v/v paraffin oil yielded an improved titer of 7.2 ± 0.29 g L^{-1} after 136 h of cultivation. With further increase in the concentration of paraffin oil to 10 % v/v, the biomass titer reduced marginally to 7 ± 0.31 g L^{-1} (Fig. 4a). Similar observations have also been reported by Han et al. (2009), where at the end of 170 h of cultivation of *M. trichosporium*, the biomass titer obtained in the control was 2 g L^{-1}, which increased to 6 g L^{-1} with the addition of 5 % v/v paraffin oil, and dropped to 1.8 g L^{-1} with further increase in the concentration to 10 % v/v. These observations point towards the improved performance of *M. trichosporium* in the present study in airlift reactor under similar concentrations of paraffin oil. Furthermore, the biomass titer improved with the increase in the concentration of silicone oil from 5 % v/v, and reached a maximum titer of 7.68 ± 0.31 g L^{-1} at 10 % v/v (Fig. 4a). Thus, under the supplementation of 10 % v/v silicone oil, the biomass titer achieved for *M. trichosporium* in airlift reactor was significantly higher than that obtained for methanotrophic consortium (0.004×10^{-9} g L^{-1}) in two-phase partition trickling bed reactor (Rocha-Rios et al., 2009).

Furthermore, the performance characteristics of the airlift reactor also improved under the chosen concentration of the mass transfer vector. For instance, with the addition of 10 % v/v silicone oil, the highest values of k_La obtained for oxygen and methane in airlift reactor were 98.5 ± 2.5 and 87.5 ± 2.2 h^{-1}, respectively (Fig. 4b), which were remarkably higher than that obtained for stirred tank reactor (0.011 s^{-1} or 39.6 h^{-1}) operated at 500 rpm with the same concentration of silicone oil (Rocha-Rios et al., 2010). Similarly, the maximum biomass productivity and methane fixation rate with 10 % v/v silicone oil were estimated to be 1.46 ± 0.04 and 0.80 ± 0.02 g L^{-1} d^{-1}, respectively (Fig. 4c). As compared to aqueous mineral salt media, mass transfer vectors have been reported to possess greater affinity for oxygen and methane (Rocha-Rios et al., 2009). The addition of 10 % v/v silicone oil to the fermentation media resulted in 26 % increment each in $k_La_{O_2}$ and $k_La_{CH_4}$, relative to the control (without any vector supplementation). This improvement in gas-to-liquid mass transfer rate could be accountable for increase in the dissolution of gases in the fermentation media, and enhancement in the delivery of oxygen and methane to the cells thereof (Patel et al., 2020b). The improved bioavailability of these gases consequently led to increments of 20 % in biomass titer, 14.7 % in biomass productivity and 14.6 % in methane fixation rate as compared to the control. Methane available to the cells is oxidized into methanol and subsequently into formaldehyde, formic acid, and CO_2. Biomass formation occurs as result of the assimilation of a part of the intermediately produced formate or formaldehyde as carbon source via RuMP or serine pathway (Sahoo et al., 2021). Therefore, in addition to mass

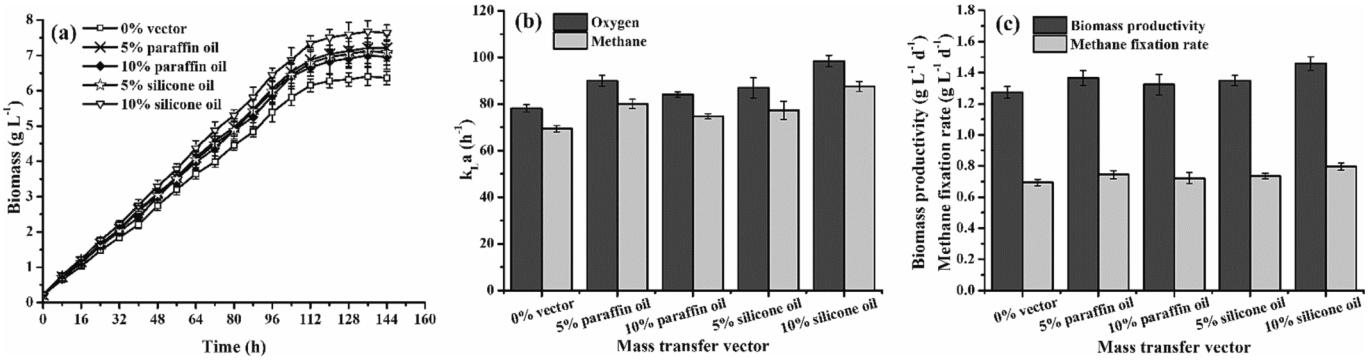

Fig. 4. (a) Biomass titer, (b) volumetric mass transfer coefficient for oxygen ($k_La_{O_2}$) and volumetric mass transfer coefficient for methane ($k_La_{CH_4}$) and (c) biomass productivity and methane fixation rate obtained in airlift reactor with varying concentrations of different mass transfer vectors. Significant differences ($p \leq 0.05$) were noted through statistical analysis using one-way ANOVA.

transfer, biomass production is also influenced by the activities of the respective enzymes (MMO, MDH and formaldehyde dehydrogenase) responsible for the production and assimilation of formaldehyde/formate.

This is the first study presenting a combinatorial approach of design of micro-sparger, engagement of draft tube and supplementation of mass transfer vector in an airlift reactor towards achieving improved biomass production and methane sequestration in methanotrophic cultivation system. Altogether, under the application of these specified process engineering strategies in airlift reactor, the present study showed an improvement of 126 % in biomass titer, 143 % biomass productivity, and 148 % in methane fixation rate, as compared to the previous work carried out in a semi-batch stirred tank reactor (Sahoo et al., 2022). In general, airlift reactors are preferable over stirred tank reactors owing to the absence of mechanical moving parts, and thereby providing a low shear stress environment for cultivation of cells, accompanied by the advantage of relatively minimal energy requirement (Lechowska et al., 2019; Teli and Mathpati, 2021). Moreover, airlift reactors have been reported to exhibit better performance as compared to stirred tank reactors particularly in case of high cell density cultures which are susceptible to poor mixing and mass transfer limitations (AL-Mashhadani et al., 2015). For instance, under selected process parameters in internal loop airlift reactor (present study), the highest $k_La_{CH_4}$ ($87.5 \pm 2.2\ h^{-1}$) attained was 460-folds greater than that was previously estimated in case of semi-batch stirred tank reactor ($0.19\ h^{-1}$) (Sahoo et al., 2022). In addition to $k_La_{CH_4}$, the highest value of $k_La_{O_2}$ ($98.5 \pm 2.5\ h^{-1}$) achieved in this study was also found to be higher than trickle-bed reactor ($k_La_{O_2}$: $9.54\ h^{-1}$, Sheets et al., 2017) and methane transfer chamber coupled-external loop airlift reactor ($k_La_{O_2}$: $97.2\ h^{-1}$, $k_La_{CH_4}$: $70.8\ h^{-1}$, Ghaz-Jahanian et al., 2018), reported for the cultivation of methanotrophs to produce methanol through biological oxidation of methane.

3.2. Process engineering strategies for improved methanol production in second stage

The effect of elevated pressure on methanol production from CO_2 was investigated under varying absolute pressure in the reactor headspace ranging from 1 to 5 bar. The methanol concentration was observed to increase concomitantly with the increase in absolute pressure from 1 bar, and attained a maximum value of 1.98 ± 0.08 g/L (61.8 ± 2.5 mM) at 4 bar (Fig. 5), which was a 235.6 % increment over the titer obtained under atmospheric pressure (0.59 ± 0.03 g/L). This remarkable improvement in methanol titer could be attributed to the increase in the availability of CO_2 in the media under elevated pressure condition. Authors have reported that elevated pressure can exert significant impact on microbial cells at molecular level including enzymatic activity, cell permeability, protein structure and synthesis of metabolic products (Amulya et al., 2020). This in turn can potentially induce the development of specific genetic, physiological and/or metabolic phenotypes in the microorganism, with consequent effect on the pattern of product formation. Stoichiometrically, one mole of CO_2 can produce one mole of methanol. So, when 50 % v/v CO_2 concentration is maintained inside the 2 L reactor (with 90 % headspace volume), the amount of CO_2 fed equals to 160.7 mmol (7.07 g). Theoretically, this can produce 160.7 mmol of methanol. However, the observed yield of methanol was 1.98 g/L (corresponding to an amount of 0.4 g or 12.5 mmol) (see supplementary materials). Based on the amount of methanol produced, the percentage of CO_2 fixed (as extracellularly secreted methanol) at 4 bar was estimated to be 7.7 %. This could be attributed to the utilization of remaining CO_2 as formate, formaldehyde or methanol (formed via reduction), and assimilation into the biomass towards cell maintenance. Another possibility might be the limited biocatalytic potential of the cells to reduce CO_2 in reverse direction of equilibrium.

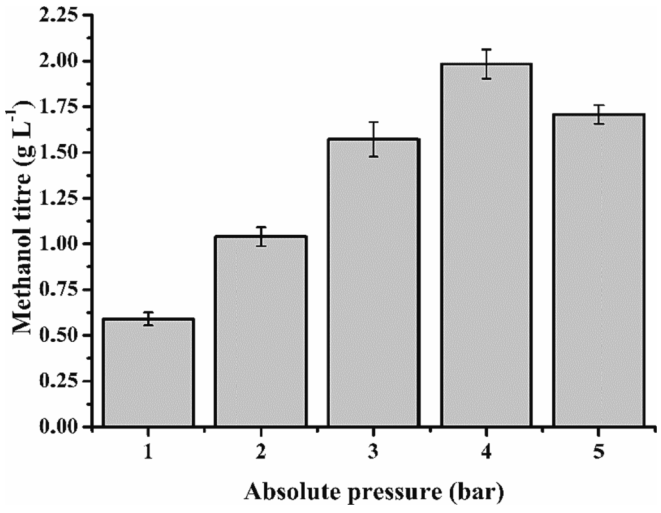

Fig. 5. Methanol titer under varying operating pressures in high-pressure stirred tank reactor. Significant differences ($p \leq 0.05$) were noted through statistical analysis using one-way ANOVA.

Researchers have reported similar studies demonstrating the effect of elevated pressure on product metabolism in other microbial systems. Kim et al. (2017) reported a threefold increment in H_2 production from carbon monoxide at 4 bar in *Thermococcus onnurineus* NA1. Roger et al. (2018) reported 20-fold increase in formate production from a mixture of CO_2 and H_2 at 10 bar in genetically modified *Escherichia coli* K12. Lopes et al. (2009) reported 3.7-fold enhancement in lipase productivity at 5 bar in *Yarrowia lipolytica* W29. However, this is first study investigating the effect of elevated pressure on methanol production from CO_2 using methanotrophic biomass as biocatalyst.

Further increase in the absolute pressure above 4 bar resulted in significant reduction in methanol titer to 1.7 ± 0.05 g/L. This observation could be attributed to the integrated effect of high pressure and high volume of CO_2 available per unit volume of the methanotrophic culture, imposing plausible inhibitory effect on electron transport chain, carbon metabolism and enzyme activity (Sahoo et al., 2022). In general, higher CO_2 pressure beyond 4–5 bar has been reported to hinder the cell viability in certain Type II methanotrophic species (Wendlandt et al., 1993). Moreover, *M. trichosporium* specifically being a Gram-negative organism is possibly more vulnerable to phospholipid solubilisation in the cell membrane due to the lack of thick peptidoglycan layer under higher CO_2 pressure stress (Schulz et al., 2012). Methanol titer was found to increase gradually till 24th h of the batch, after which a slight decline was observed. This could be attributed to the exhaustion of endogenous reducing equivalents (*e.g.,* NADH and PHB), or methanol degradation owing to enzymatic or non-enzymatic interactions (Xin et al., 2007). Biomass density almost remained constant in the pressure range of 1 to 4 bar. However, it was observed to decline slightly at 5 bar with the progression of the batch, which could be another possible reason for reduced methanol titer at this pressure (see supplementary materials).

There are very few studies reporting the production of methanol from the reduction of CO_2 in methanotrophs under atmospheric pressure (Patel et al., 2016a; Xin et al., 2007). A previous study reported a maximum methanol titer of 0.58 g/L (18.10 mM) using *Methylosinus trichosporium* as biocatalyst, which was till date the highest methanol titer achieved through biological CO_2 reduction pathway (Sahoo et al., 2022). In the present study, the elevation of operating pressure up to 4 bar resulted in further 3.4-fold increment in methanol production as compared to the previous report.

Methanol production through CO_2 reduction is carried out in phosphate buffer medium to resist major changes in pH resulting from CO_2 solubility (Sahoo et al., 2022; Patel et al., 2016a; Xin et al., 2007). In the present study, the initial and final pH (at the end of the batch) of the culture were found to decrease from 6.8 ± 0.14 to 6.65 ± 0.13, and 6.56 ± 0.1 to 6.14 ± 0.09, respectively, with the increase in pressure from 1

bar to 5 bar (see supplementary materials). The slight decrease in pH with the progression of the batch and the increase in pressure, could be attributed to the increase in solubility of CO_2. However, the use of buffer did help in resisting sharp and major decline in pH with the increasing CO_2 solubility.

Alternatively, authors have reported the production of methanol through biological oxidation of methane by methanotrophs. However, this specific route is constrained by further sequential oxidation of the produced methanol into subsequent intermediate metabolites, and the requirement for methanol dehydrogenase inhibitors and formate to achieve extracellular secretion of methanol into the media (Sahoo et al., 2022). Despite several attempts to enhance methanol production via biological oxidation of methane, the maximum methanol titer achieved is limited to a range of 5.37–52.9 mM (0.17–1.69 g/L) (Patel et al., 2020a, 2016a). Duan et al. (2011) reported a maximum methanol titer of 1.12 g/L and $Y_{p/x}$ (methanol yield coefficient relative to biomass) of 0.066, through biological oxidation of methane using a very high biomass density of *M. trichosporium* (17 g/L dry cell weight), high concentrations of methanol dehydrogenase inhibitors (400 mM phosphate and 10 mM $MgCl_2$) and paraffin oil as mass transfer vector. Another study reported the production of methanol from methane through covalent immobilisation of *Methylocystis bryophila* cells on coconut coir using paraffin oil as mass transfer vector (Patel et al., 2020a). The subsequent application of repeated batch strategy to this process resulted in a maximum cumulative methanol accumulation of 52.9 mM (1.69 g/L), with a $Y_{p/x}$ value of 0.56 at the end of eight cycles of biomass reutilisation. On the contrary, the $Y_{p/x}$ in stirred tank reactor, operated in batch mode at 4 bar, was estimated to be 0.6 in the present study, signifying the ameliorated performance of the organism under elevated operating pressure, which is a much simpler strategy relative to other contemporary approaches. Therefore, in the current study, the methanol production attained through biological CO_2 reduction, both in terms of titer and yield, was found to be much higher than other studies reported in literature concerned with biological methane oxidation. A comparative table for methanol production under different process conditions and reactor types has been provided (see supplementary materials).

Biocatalytic activity of methanotrophic enzymes plays a vital role in determining the bioconversion yield of greenhouse gases to methanol. Increased methanol production from methane oxidation is associated with higher activity of MMO and reduced activity of MDH to facilitate the oxidation of methane to methanol, and limit the sequential oxidation of methanol into other intermediate metabolites, respectively. For instance, Patel et al. (2020a) correlated the enhanced methanol production in *M. bryophila* cells under optimum conditions with increased relative MMO activity of 108 % and decreased relative MDH activity of 91.4 % compared to control (100 %). However, there are no studies reporting the activities of methanotrophic enzymes for methanol production through CO_2 reduction pathway (in the absence of methane). Improved methanol production from CO_2 have been suggested to require higher activities of formate-, formaldehyde- and methanol dehydrogenase enzymes to accomplish the reduction of CO_2 into methanol (Patel et al., 2016a; Xin et al. 2007).

Authors have reported several approaches towards the enhancement of methanol production from greenhouse gases, such as, co-cultivation of methanotrophs, cell immobilization on various supports (*e.g.*, polymers containing magnetic nanoparticles, banana leaves and coconut coir), and repeated-batch cultivation (Patel et al., 2022, 2021, 2020a). Moreover, authors have reported the use of biogas derived from dark fermentation and anaerobic digestion of bio-wastes, such as, potato peels and wheat straw, to reduce the cost associated with the utilization of pure gases as methanotrophic feed (Patel et al., 2023, 2022, 2021). However, to the best knowledge of the authors, this is the first study demonstrating the effect of elevated pressure on methanol production using methanotrophic bacteria as biocatalyst.

Researchers have been working on different aspects of bioprocess to improve its economic feasibility at pilot scale. For instance, authors have reported the use of cheaper supports for cell immobilization, such as, banana leaves and coconut coir (Patel et al., 2021; 2020a). Similarly, biogas derived from anaerobic digestion of bio-wastes has been reported as an alternative feed to expensive pure gases (Patel et al. 2023). In the present study, an airlift reactor and a high-pressure stirred tank reactor have been designed. These could further be scaled-up for pilot-scale studies in potential industries such as oil–gas extraction, refineries, gas processing industries and chemical plants where large amounts of off-gases containing methane and CO_2 are available. The present study can offer a potential technology which can be an ideal solution to the industries, offering simultaneous sequestration of greenhouse gases and value-addition through methanol production. Moreover, the two reactors are designed to operate at room temperature, thus cutting-down the cost associated with maintenance of temperature, without compromising in yield and productivity. Economic feasibility can further be enhanced at pilot-scale through recycling of un-utilized methane and biomass in the first and second stages, respectively, of the two-stage integrated bioprocess.

4. Conclusions

A combinatorial process engineering strategy was employed to two-stage integrated bioprocess for improved methanol production using *M. trichosporium*. Use of micro-sparger, engagement of draft tube and supplementation of mass transfer vector in airlift reactor addressed the key challenge of mass transfer and solubility limitations of methane in the first stage. Biomass titer, biomass productivity and methane fixation rate were improved by 126 %, 143 % and 148 %, respectively, compared with the two-stage process without process engineering strategy. In the second stage, elevation of headspace pressure in reactor increased CO_2 solubility, leading to 235.6 % increment in methanol titer, relative to atmospheric pressure.

CRediT authorship contribution statement

Krishna Kalyani Sahoo: Reactor design, experimentation, formal analysis and interpretation of data, and writing - original draft. **Ankan Sinha:** Conceptualization. **Debasish Das:** Conceptualization, Supervision, Writing - review & editing.

Declaration of Competing Interest

The authors declare that they have no known competing financial interests or personal relationships that could have appeared to influence the work reported in this paper.

Data availability

Data will be made available on request.

Acknowledgements

Krishna Kalyani Sahoo is grateful to Ministry of Education, Government of India for her research fellowship.

Appendix A. Supplementary data

Supplementary data to this article can be found online at https://doi.org/10.1016/j.biortech.2023.128603.

References

AL-Mashhadani, M.K.H., Wilkinson, S.J., Zimmerman, W.B., 2015. Airlift bioreactor for biological applications with microbubble mediated transport processes. Chem. Eng. Sci. 137, 243–253.

Amulya, K., Kopperi, H., Venkata Mohan, S., 2020. Tunable production of succinic acid at elevated pressures of CO2 in a high pressure gas fermentation reactor. Bioresour. Technol. 309, 123327 https://doi.org/10.1016/J.BIORTECH.2020.123327.
Doran, P.M., 1995. Bioprocess Engineering Principles, second ed. Elsevier.
Duan, C., Luo, M., Xing, X., 2011. High-rate conversion of methane to methanol by Methylosinus trichosporium OB3b. Bioresour. Technol. 102, 7349–7353. https://doi.org/10.1016/J.BIORTECH.2011.04.096.
Duan, Y., Shi, F., 2014. Bioreactor design for algal growth as a sustainable energy source. React. Process Des. Sustain. Energy Technol. 27–60 https://doi.org/10.1016/B978-0-444-59566-9.00002-8.
Ghaz-Jahanian, M.A., Khoshfetrat, A.B., Hosseinian Rostami, M., Haghighi, M., 2018. An innovative bioprocess for methane conversion to methanol using an efficient methane transfer chamber coupled with an airlift bioreactor. Chem. Eng. Res. Des. 134, 80–89. https://doi.org/10.1016/J.CHERD.2018.03.039.
Han, B., Su, T., Wu, H., Gou, Z., Xing, X.H., Jiang, H., Chen, Y., Li, X., Murrell, J.C., 2009. Paraffin oil as a "methane vector" for rapid and high cell density cultivation of methylosinus trichosporium OB3b. Appl. Microbiol. Biotechnol. 83, 669–677. https://doi.org/10.1007/S00253-009-1866-2.
Hanotu, J.O., Bandulasena, H., Zimmerman, W.B., 2017. Aerator design for microbubble generation. Chem. Eng. Res. Des. 123, 367–376. https://doi.org/10.1016/J.CHERD.2017.01.034.
Hekmat, A., Amooghin, A.E., Moraveji, M.K., 2010. CFD simulation of gas–liquid flow behaviour in an air-lift reactor: determination of the optimum distance of the draft tube. Simul. Model. Pract. Theory 18, 927–945. https://doi.org/10.1016/J.SIMPAT.2010.02.009.
Kim, M.S., Fitriana, H.N., Kim, T.W., Kang, S.G., Jeon, S.G., Chung, S.H., Park, G.W., Na, J.G., 2017. Enhancement of the hydrogen productivity in microbial water gas shift reaction by Thermococcus onnurineus NA1 using a pressurized bioreactor. Int. J. Hydrogen Energy 42, 27593–27599. https://doi.org/10.1016/J.IJHYDENE.2017.07.024.
Lechowska, J., Kordas, M., Konopacki, M., Fijałkowski, K., Drozd, R., Rakoczy, R., 2019. Hydrodynamic studies in magnetically assisted external-loop airlift reactor. Chem. Eng. J. 362, 298–309. https://doi.org/10.1016/J.CEJ.2019.01.037.
Li, X., Chen, Y., Zheng, Z., Gao, M., Wang, Z., Zhang, K., Liu, H., Zhan, X., 2020. Power-saving airlift bioreactor with helical sieve plates: Developmental and performance studies. Chem. Eng. Res. Des. 158, 1–11. https://doi.org/10.1016/J.CHERD.2020.03.014.
Lopes, M., Gomes, N., Mota, M., Belo, I., 2009. Yarrowia lipolytica growth under increased air pressure: Influence on enzyme production. Appl. Biochem. Biotechnol. 159, 46–53. https://doi.org/10.1007/S12010-008-8359-0/FIGURES/4.
Lucile, F., Cézac, P., Contamine, F., Serin, J.P., Houssin, D., Arpentinier, P., 2012. Solubility of carbon dioxide in water and aqueous solution containing sodium hydroxide at temperatures from (293.15 to 393.15) K and pressure up to 5 MPa: experimental measurements. J. Chem. Eng. Data 57, 784–789. https://doi.org/10.1021/JE200991X/ASSET/IMAGES/LARGE/JE-2011-00991X_0011.JPEG.
Lueske, J., Kar, K., Piras, L., Pressler, J., 2015. Power draw and gas-liquid mass transfer characteristics of a stirred-tank reactor with draft tube configuration. Chem. Eng. Technol. 38, 1993–2001. https://doi.org/10.1002/CEAT.201500071.
Lukić, N.L., Šijački, I.M., Kojić, P.S., Popović, S.S., Tekić, M.N., Petrović, D.L., 2017. Enhanced mass transfer in a novel external-loop airlift reactor with self-agitated impellers. Biochem. Eng. J. 118, 53–63. https://doi.org/10.1016/J.BEJ.2016.11.014.
Luo, L., Liu, F., Xu, Y., Yuan, J., 2011. Hydrodynamics and mass transfer characteristics in an internal loop airlift reactor with different spargers. Chem. Eng. J. 175, 494–504. https://doi.org/10.1016/J.CEJ.2011.09.078.
Patel, S.K.S., Gupta, R.K., Kalia, V.C., Lee, J.K., 2022. Synthetic design of methanotroph co-cultures and their immobilization within polymers containing magnetic nanoparticles to enhance methanol production from wheat straw-based biogas. Bioresour. Technol. 364, 128032 https://doi.org/10.1016/J.BIORTECH.2022.128032.
Patel, S.K.S., Gupta, R.K., Kalia, V.C., Lee, J.K., 2021. Integrating anaerobic digestion of potato peels to methanol production by methanotrophs immobilized on banana leaves. Bioresour. Technol. 323, 124550 https://doi.org/10.1016/J.BIORTECH.2020.124550.
Patel, S.K.S., Kalia, V.C., Joo, J.B., Kang, Y.C., Lee, J.K., 2020a. Biotransformation of methane into methanol by methanotrophs immobilized on coconut coir. Bioresour. Technol. 297, 122433 https://doi.org/10.1016/J.BIORTECH.2019.122433.
Patel, S.K.S., Kalia, V.C., Lee, J.K., 2023. Integration of biogas derived from dark fermentation and anaerobic digestion of biowaste to enhance methanol production by methanotrophs. Bioresour. Technol. 369, 128427 https://doi.org/10.1016/J.BIORTECH.2022.128427.
Patel, S.K.S., Mardina, P., Kim, D., Kim, S.Y., Kalia, V.C., Kim, I.W., Lee, J.K., 2016a. Improvement in methanol production by regulating the composition of synthetic gas mixture and raw biogas. Bioresour. Technol. 218, 202–208. https://doi.org/10.1016/J.BIORTECH.2016.06.065.
Patel, S.K.S., Selvaraj, C., Mardina, P., Jeong, J.H., Kalia, V.C., Kang, Y.C., Lee, J.K., 2016b. Enhancement of methanol production from synthetic gas mixture by Methylosinus sporium through covalent immobilization. Appl. Energy 171, 383–391. https://doi.org/10.1016/j.apenergy.2016.03.022.
Patel, S.K.S., Shanmugam, R., Kalia, V.C., Lee, J.K., 2020b. Methanol production by polymer-encapsulated methanotrophs from simulated biogas in the presence of methane vector. Bioresour. Technol. 304, 123022 https://doi.org/10.1016/J.BIORTECH.2020.123022.
Pruteanu, C.G., Ackland, G.J., Poon, W.C.K., Loveday, J.S., 2017. When immiscible becomes miscible—methane in water at high pressures. Sci. Adv. 3 https://doi.org/10.1126/SCIADV.1700240.
Rasouli, Z., Valverde-Pérez, B., D'Este, M., De Francisci, D., Angelidaki, I., 2018. Nutrient recovery from industrial wastewater as single cell protein by a co-culture of green microalgae and methanotrophs. Biochem. Eng. J. 134, 129–135. https://doi.org/10.1016/J.BEJ.2018.03.010.
Rocha-Rios, J., Bordel, S., Hernández, S., Revah, S., 2009. Methane degradation in two-phase partition bioreactors. Chem. Eng. J. 152, 289–292. https://doi.org/10.1016/J.CEJ.2009.04.028.
Rocha-Rios, J., Muñoz, R., Revah, S., 2010. Effect of silicone oil fraction and stirring rate on methane degradation in a stirred tank reactor. J. Chem. Technol. Biotechnol. 85, 314–319. https://doi.org/10.1002/JCTB.2339.
Rocha-Rios, J., Quijano, G., Thalasso, F., Revah, S., Muñoz, R., 2011. Methane biodegradation in a two-phase partition internal loop airlift reactor with gas recirculation. J. Chem. Technol. Biotechnol. 86, 353–360. https://doi.org/10.1002/JCTB.2523.
Roger, M., Brown, F., Gabrielli, W., Sargent, F., 2018. Efficient hydrogen-dependent carbon dioxide reduction by Escherichia coli. Curr. Biol. 28, 140–145.e2. https://doi.org/10.1016/J.CUB.2017.11.050.
Sahoo, K.K., Datta, S., Goswami, G., Das, D., 2022. Two-stage integrated process for bio-methanol production coupled with methane and carbon dioxide sequestration: kinetic modelling and experimental validation. J. Environ. Manage. 301, 113927 https://doi.org/10.1016/J.JENVMAN.2021.113927.
Sahoo, K.K., Goswami, G., Das, D., 2021. Biotransformation of methane and carbon dioxide into high-value products by methanotrophs: current state of art and future prospects. Front. Microbiol. 12 https://doi.org/10.3389/FMICB.2021.636486.
Schulz, A., Vogt, C., Richnow, H.H., 2012. Effects of high CO2 concentrations on ecophysiologically different microorganisms. Environ. Pollut. 169, 27–34. https://doi.org/10.1016/J.ENVPOL.2012.05.010.
Sheets, J.P., Lawson, K., Ge, X., Wang, L., Yu, Z., Li, Y., 2017. Development and evaluation of a trickle bed bioreactor for enhanced mass transfer and methanol production from biogas. Biochem. Eng. J. 122, 103–114. https://doi.org/10.1016/j.bej.2017.03.006.
Tang, Y., Huang, Y., Gan, W., Xia, A., Liao, Q., Zhu, X., 2021. Ethanol production from gas fermentation: Rapid enrichment and domestication of bacterial community with continuous CO/CO2 gas. Renew. Energy 175, 337–344. https://doi.org/10.1016/J.RENENE.2021.04.134.
Teli, S.M., Mathpati, C.S., 2021. Experimental and numerical study of gas-liquid flow in a sectionalized external-loop airlift reactor. Chin. J. Chem. Eng. 32, 39–60. https://doi.org/10.1016/J.CJCHE.2020.10.023.
Van Hecke, W., Bockrath, R., De Wever, H., 2019. Effects of moderately elevated pressure on gas fermentation processes. Bioresour. Technol. 293, 122129 https://doi.org/10.1016/J.BIORTECH.2019.122129.
Verhelst, S., Turner, J.W., Sileghem, L., Vancoillie, J., 2019. Methanol as a fuel for internal combustion engines. Prog. Energy Combust. Sci. 70, 43–88. https://doi.org/10.1016/j.pecs.2018.10.001.
Wendlandt, K.-D., Jechorek, M., Brühl, E., 1993. The influence of pressure on the growth of methanotrophic bacteria. Acta Biotechnol. 13, 111–115. https://doi.org/10.1002/ABIO.370130205.
Xin, J.Y., Zhang, Y.X., Zhang, S., Xia, C.G., Li, S.B., 2007. Methanol production from CO2 by resting cells of the methanotrophic bacterium Methylosinus trichosporium IMV 3011. J. Basic Microbiol. 47, 426–435. https://doi.org/10.1002/JOBM.200710313.
Zhang, T., Wang, X., Zhou, J., Zhang, Y., 2018. Enrichments of methanotrophic–heterotrophic cultures with high poly-β-hydroxybutyrate (PHB) accumulation capacities. J. Environ. Sci. 65, 133–143. https://doi.org/10.1016/J.JES.2017.03.016.
Zhang, T., Zhou, J., Wang, X., Zhang, Y., 2017. Coupled effects of methane monooxygenase and nitrogen source on growth and poly-β-hydroxybutyrate (PHB) production of Methylosinus trichosporium OB3b. J. Environ. Sci. (China) 52, 49–57. https://doi.org/10.1016/J.JES.2016.03.001.
Zhao, Y., Cimpoia, R., Liu, Z., Guiot, S.R., 2011. Kinetics of CO conversion into H 2 by Carboxydothermus hydrogenoformans. Appl. Microbiol. Biotechnol. 91, 1677–1684. https://doi.org/10.1007/S00253-011-3509-7/TABLES/1.

Web references

Global Methane Tracker, 2022. International Energy Agency. https://www.iea.org/reports/global-methane-tracker-2022/overview. (Accessed 20 December 2022). accessed.
International Energy Agency, 2022. https://www.iea.org/news/global-co2-emissions-rebounded-to-their-highest-level-in-history-in-2021. (Accessed 20 December 2022). accessed.

Further readings

Kim, H.G., Han, G.H., Kim, S.W., 2010. Optimization of lab scale methanol production by methylosinus trichosporium OB3b. Biotechnol. Bioprocess Eng. 15, 476–480. https://doi.org/10.1007/S12257-010-0039-6/METRICS.
Kulkarni, P.P., Khonde, V.K., Deshpande, M.S., Sabale, T.R., Kumbhar, P.S., Ghosalkar, A. R., 2021. Selection of methanotrophic platform for methanol production using methane and biogas. J. Biosci. Bioeng. 132, 460–468. https://doi.org/10.1016/J.JBIOSC.2021.07.007.
Patel, S.K.S., Kondaveeti, S., Otari, S.V., Pagolu, R.T., Jeong, S.H., Kim, S.C., Cho, B.K., Kang, Y.C., Lee, J.K., 2018. Repeated batch methanol production from a simulated biogas mixture using immobilized Methylocystis bryophila. Energy 145, 477–485. https://doi.org/10.1016/J.ENERGY.2017.12.142.